

Number counts and clustering properties of bright distant red galaxies in the UKIDSS Ultra Deep Survey Early Data Release

S. Foucaud,^{1*} O. Almaini,¹ I. Smail,² C. J. Conselice,¹ K. P. Lane,¹ A. C. Edge,² C. Simpson,³ J. S. Dunlop,⁴ R. J. McLure,⁴ M. Cirasuolo,⁴ P. Hirst,⁵ M. G. Watson⁶ and M. J. Page⁷

¹*School of Physics and Astronomy, University of Nottingham, University Park, Nottingham NG7 2RD*

²*Institute for Computational Cosmology, Department of Physics, Durham University, South Road, Durham DH1 3LE*

³*Astrophysics Research Institute, Liverpool John Moores University, Egerton Wharf, Birkenhead CH41 1LD*

⁴*SUPA† Institute for Astronomy, University of Edinburgh, Royal Observatory, Edinburgh EH9 3HJ*

⁵*Joint Astronomy Centre, 660 N. A‘ohōkū Place, University Park, Hilo, Hawaii 96720, USA*

⁶*X-ray Astronomy Group, Department of Physics and Astronomy, University of Leicester, Leicester LE1 7RH*

⁷*Mullard Space Science Laboratory, University College London, Holmbury St Mary, Dorking, Surrey RH5 6NT*

Accepted 2006 December 15. Received 2006 December 12; in original form 2006 June 14

ABSTRACT

We describe the number counts and spatial distribution of 239 distant red galaxies (DRGs), selected from the Early Data Release of the UKIDSS Ultra Deep Survey. The DRGs are identified by their very red infrared colours with $(J - K)_{AB} > 1.3$, selected over 0.62 deg^2 to a 90 per cent completeness limit of $K_{AB} \simeq 20.7$. This is the first time that a large sample of bright DRGs has been studied within a contiguous area, and we provide the first measurements of their number counts and clustering. The population shows strong angular clustering, intermediate between those of K -selected field galaxies and optical/infrared-selected extremely red galaxies. Adopting the redshift distributions determined from other recent studies, we infer a high correlation length of $r_0 \sim 11 h^{-1} \text{ Mpc}$. Such strong clustering could imply that our galaxies are hosted by very massive dark matter haloes, consistent with the progenitors of present-day $L \gtrsim L_*$ elliptical galaxies.

Key words: galaxies: evolution – galaxies: high-redshift – cosmology: observations.

1 INTRODUCTION

A new near-infrared selection technique has been developed in recent years to sample galaxies in the high-redshift Universe. By relying on purely near-infrared colours, this potentially avoids many biases which are inherent in optical techniques, particularly for detected dusty and/or evolved galaxies. Franx et al. (2003) argue that the simple $(J - K)_{AB} > 1.3$ colour selection criterion produces a sample that is mainly populated by galaxies at $z > 2$, at least at faint K -band magnitudes ($K_{AB} \gtrsim 21$). These are the so-called distant red galaxies (hereafter DRGs). In the Faint Infrared Extragalactic Survey (FIRES), Franx et al. (2003) selected 14 candidate galaxies at $z > 2$ to a depth of $K_{AB} < 24.4$, of which six were spectroscopically confirmed (van Dokkum et al. 2003). Labbé et al. (2005) found that approximately 70 per cent of DRGs are dusty star-forming galaxies and the remaining 30 per cent are passively evolved galaxies.

Work by Rudnick et al. (2003) suggests that DRGs may be a significant constituent of the $z \sim 2$ – 3 Universe in terms of stellar

mass. Förster Schreiber et al. (2004) demonstrated that the average rest-frame optical colours of DRGs fall within the range covered by normal galaxies locally, unlike the Lyman-break galaxies (LBGs – Steidel et al. 1996) which are typically much bluer. Larger samples of DRGs covering a wide range in stellar mass are now required to understand fully the importance of this population. In particular, studies conducted so far have (by necessity) concentrated on DRGs selected over relatively small areas, and very little is known about the bright end of this population.

In terms of stellar mass, metallicity and star formation rate, Reddy et al. (2005) find strong similarities between optically selected and near-infrared selected galaxy samples. Clustering offers an alternative way to study these populations. At large scales, the galaxy distribution is dominated by dark matter halo clustering, which is a strong function of halo mass. Several studies have measured high clustering strength for high-redshift galaxies selected in the near-infrared ($r_0 = 10$ – $15 h^{-1} \text{ Mpc}$) (Daddi et al. 2003; Grazian et al. 2006), comparable to the most luminous galaxies in the local Universe.

In this paper we present a study of the first large sample of DRGs selected at bright infrared magnitudes ($K_{AB} < 21$) in a contiguous area. We analyse the number counts and clustering and draw

*E-mail: Sebastien.Foucaud@nottingham.ac.uk

†Scottish Universities Physics Alliance.

conclusions about their likely origin. Throughout this paper, we assume $\Omega_m = 0.3$, $\Omega_\Lambda = 0.7$ and $h = H_0/70 \text{ km s}^{-1} \text{ Mpc}^{-1}$.

2 THE UKIDSS ULTRA DEEP SURVEY EARLY DATA RELEASE

2.1 Survey and Early Data Release

The UKIRT Infrared Deep Sky Survey (UKIDSS – Lawrence et al. 2006)¹ began observations in the spring of 2005, using the Wide-Field Camera (WFCAM – Casali et al., in preparation) at the 3.8-m United Kingdom InfraRed Telescope (UKIRT). Comprising five sub-surveys, it will take 7 years to complete and will cover a range of areas and depths. The deepest of these five sub-surveys, the Ultra Deep Survey (UDS), aims to cover 0.8 deg^2 to a depth of $K_{AB} = 25.0$, $H_{AB} = 25.4$, $J_{AB} = 26.0$ (5σ , point-source). It is centred on the *Subaru/XMM-Newton* Deep Survey field (SXDS – Sekiguchi et al. 2005) at $02^{\text{h}}18^{\text{m}}00^{\text{s}}$, $-05^{\circ}00'00''$ (J2000).

Since 2006 February 10, the UKIDSS Early Data Release (EDR) has been available to the European Southern Observatory (ESO) community.² A full description of this data release is given in Dye et al. (2007).

2.2 Image stacking and mosaics

The stacking of the UDS EDR data was performed by our team using a slightly different recipe from the standard UKIDSS pipeline. Given the (relatively) small size of the field, it is possible to create a full mosaic before extracting catalogues, rather than merge catalogues extracted from individual chips. Given the various jitter and offset sequences, this helps to optimize depth in overlap regions and to produce a more homogeneous final image.

Each observation block consists of a 4-point mosaic to tile the 0.8-deg^2 field, producing 16 images each of $\simeq 15$ min exposure (see Dye et al. 2007). Individual reduced frames for each observation block were extracted from the UKIDSS pipeline as the starting point for our final mosaicked stack (including astrometric and photometric solutions). We used the variance map produced by the pipeline to weight each frame before stacking and rescaled the pixel flux for each individual image using the pipeline zero-points. The stacking was carried out in a two-step process by using the SWARP software, an image resampling tool (Bertin et al. 2002). The final mosaicked images in the J and K bands have the same pixel scale of 0.1342 arcsec , with identical field centres and image scales to simplify catalogue extraction. The resulting images were visually inspected, and bad regions were masked out (areas around saturated stars, cosmetic problem areas, and low signal-to-noise ratio borders). After masking, the usable area of this frame with uniform coverage is 0.62 deg^2 . We note that this is smaller than the expected 0.8-deg^2 mosaic since the UDS field centre was moved by ~ 8 arcmin shortly after observations began (to allow the use of brighter guide stars).

The image seeing measured from the mosaicked images is 0.69 arcsec FWHM in K and 0.80 arcsec in J . The rms accuracy of our astrometry is $\simeq 0.05 \text{ arcsec}$ (i.e. < 1 pixel) and for our photometry the rms accuracy is $\lesssim 2$ per cent in both J and K bands (Dye et al. 2007). From direct measurements of noise in a 2-arcsec

aperture on the image we estimate 5σ limiting magnitudes of $K_{AB} = 22.5$ and $J_{AB} = 22.5$.

2.3 Catalogue extraction

We found that the standard UKIDSS source detection software did not produce optimal catalogues for the UDS. We therefore produced a much improved catalogue for the EDR by using the SExtractor software (Bertin & Arnouts 1996). The K -band image was used as the source detection image, since this is measurably deeper for most galaxy colours. All K_{AB} magnitudes quoted below are total magnitudes extracted using the SExtractor parameter MAG_AUTO, while all colour measurements are obtained from fixed 2-arcsec aperture magnitudes.

To optimize our catalogue extraction we performed a series of simulations to fine-tune the SExtractor parameters. Artificial point-like sources were added to the real K -band image using the observed point spread function (PSF) with FWHM = 0.69 arcsec (rejecting regions containing bright sources), and distributed with magnitudes in the range $14 < K_{AB} < 24$. From the resulting new image a catalogue was extracted using SExtractor and compared with the list of artificial source positions. This process was repeated 1000 times, and the resulting statistics allow us to estimate the catalogue completeness and the evolution of photometric errors. Using these simulations, SExtractor detection parameters were tuned to maximize completeness at the noise-determined 5σ depth of $K_{AB} = 22.5$, while simultaneously minimizing the number of spurious sources. While formally optimized for point-like sources, we note that these were close to optimal when we generated artificial sources using a substantially more extended PSF (FWHM = 1.2 arcsec).

Using these parameters, we extracted 78 709 sources over 0.62 deg^2 from the image, of which 34 098 were determined to be unsaturated, unmasked and from regions of uniform coverage to $K_{AB} < 22.5$. These form the basis of the analysis outlined below. Assuming that the background noise is symmetric about zero, we can estimate the spurious fraction by extracting sources from the inverted image and comparing with the number of sources extracted from the normal image. At our magnitude limit of $K_{AB} = 22.5$ the fraction of spurious detections is found to be less than 1 per cent, while the completeness level is above 70 per cent (for point sources).

3 SELECTION AND NUMBER COUNTS

3.1 Selection of DRGs

From the catalogue described above we selected objects using the $(J - K)_{AB} > 1.3$ criterion. A visual inspection of each source was then required to remove spurious detections, which at these extreme colours was found to be a relatively large fraction (~ 20 per cent). The majority are caused by diffraction spikes and cross-talk images (Dye et al. 2007) and are easy to identify and reject. This leaves 369 DRGs at $K_{AB} < 21.2$, which represents the largest sample selected over a contiguous area. The surface density derived is $n = 0.163 \pm 0.009 \text{ arcmin}^{-2}$. Fig. 1 shows the $(J - K)$ colour of these galaxies versus K -band magnitude. The object shown by a star was classified as a point-like source in our global catalogue, and is confirmed to be a star after visual inspection.

3.2 Photometric errors and contamination of DRG sample

Since our sample is based on $(J - K)$ colour selection, it is vital to carefully consider the effects of photometric errors. Since most

¹ <http://www.ukidss.org>

² <http://surveys.roe.ac.uk/wsa>

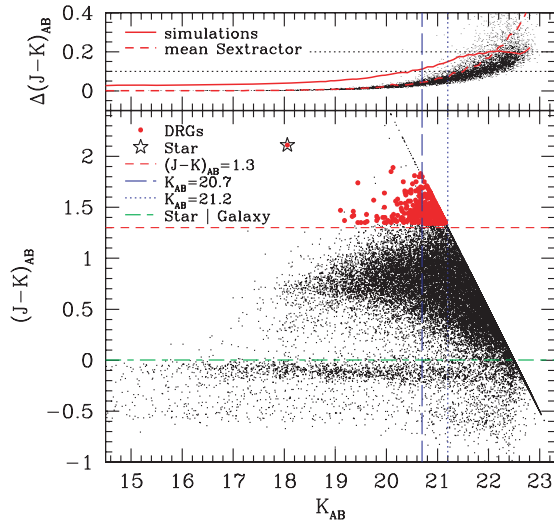


Figure 1. Lower panel: $(J - K)_{AB}$ against K_{AB} for sources in the UDS EDR field. Small points represent the full population of K -band selected objects, while larger points are those selected with $(J - K)_{AB} > 1.3$ (and visually confirmed). The colour criteria, the magnitude limit at $K_{AB} = 21.2$ and the magnitude completeness at $K_{AB} = 20.7$ are highlighted, as is the crude boundary between galaxies and the stellar locus at $(J - K)_{AB} = 0$. Upper panel: errors as derived by SExtractor on the $(J - K)_{AB}$ colours (for display purposes only one-fifth of the points are shown). Mean values are also displayed, as are errors derived from simulations.

galaxies show substantially bluer colours (Fig. 1) we can expect the number density of DRGs to be artificially boosted at fainter magnitudes, as errors push objects above the $(J - K)_{AB} > 1.3$ selection boundary. As a lower limit to this contamination we could use the photometric errors derived from SExtractor, and these are shown as a function of magnitude in Fig. 1. Our experience suggests that analytically determined errors from SExtractor are likely to be underestimates, so we use the mean photometric errors obtained from the simulations described in Section 2.3.

We use our simulated errors to estimate the contamination by randomizing the real galaxy catalogue using Monte Carlo simulations. For each object in our full catalogue, we allow the $(J - K)$ colour to vary assuming a Gaussian distribution with a standard deviation corresponding to the chosen photometric error. We then re-select our catalogue using the $(J - K)_{AB} > 1.3$ criterion, and repeat this process 1000 times. This should provide an approximate upper limit on contamination, since we are randomizing the observed galaxy catalogue (which already suffers from the effects of photometric errors).

Defining the contamination fraction from the number of objects scattered into our selection boundary minus those that are scattered out, our simulated source errors yield contamination fractions of 46.0 ± 3.8 per cent at the limiting magnitude of $K_{AB} < 21.2$, falling to 16.8 ± 3.6 per cent at $K_{AB} < 20.7$ (the estimated completeness limit; see Section 3.3). We note that the typical error on the colour is $\Delta(J - K)_{AB} \sim 0.1$ at $K_{AB} = 20.7$. As shown in Conselice et al. (2006), a slight change of the $(J - K)$ colour selection does not have a major effect on the redshift distribution.

Based on these values we conclude that our number counts and clustering measurements are reasonably robust at $K_{AB} < 20.7$, but will become increasingly unreliable at fainter magnitudes. We will therefore adopt a limit of $K_{AB} = 20.7$ for further study, which produces a sample of 239 DRGs.

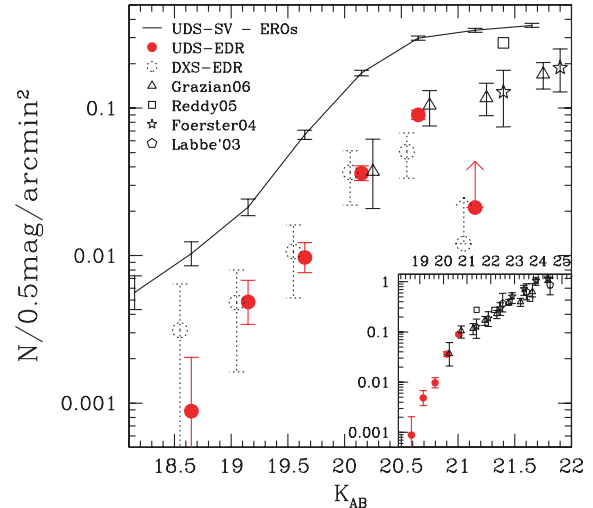


Figure 2. K -band differential number counts for our sample of DRGs. The error bars plotted are computed from Poissonian small-number statistics (Gehrels 1986). For comparison, we have overplotted the number counts for DRGs derived from the DXS EDR survey, with errors representing the field-to-field variance (see Section 3.4 – these points are slightly shifted for display purposes), and from the literature from fainter samples (Labbe et al. 2003; Förster Schreiber et al. 2004; Reddy et al. 2005; Grazian et al. 2006). ERO number counts from the UDS/DXS Science Verification (hereafter SV) sample are shown as well, for comparison. The plot inset shows number counts over a larger magnitude range.

3.3 Number counts of DRGs

Fig. 2 shows the K -band differential number counts of our sample of DRGs. The number counts indicate that our sample is complete up to approximately $K_{AB} \simeq 20.7$, after which the counts are clearly dropping. This defines our estimated completeness limit. Our simulations suggest that the contamination due to photometric errors will be ~ 16 per cent at $K_{AB} < 20.7$. We conclude that the dominant source of error in our number counts will be Poisson counting errors (plotted) and cosmic variance (discussed in Section 3.4).

At bright magnitudes (e.g. $K_{AB} < 20$) our UKIDSS data are entirely unique, and no studies exist in the literature for comparison. At fainter magnitudes, our counts are in very good agreement with the DRG counts from the Grazian et al. (2006) sample. They are also consistent with the number counts from the AEGIS survey (Foucaud et al., in preparation; see also Conselice et al. 2006). Combining literature data with the present work we can examine the global shape of the DRG number counts over a very wide dynamic range ($18.5 < K_{AB} < 25.0$). This strongly suggests a break feature in the slope at $K_{AB} \sim 20.5$ which is an effect already seen in the global K -band number counts (e.g. Gardner, Cowie & Wainscoat 1993).

We note that the projected density of DRGs is approximately 10 times lower than that of extremely red objects (hereafter EROs), and approximately 100 times lower than the global galaxy counts at a given magnitude.

3.4 Cosmic variance

As a simple test of cosmic variance, and to investigate whether the UDS is an unusual field, we used the data available from the UKIDSS Deep Extragalactic Survey (DXS) to perform a comparison study. The DXS is the other deep extragalactic component of UKIDSS (Lawrence et al. 2006), consisting of four fields with a 7-year goal of observing 35 deg^2 to depths of $K_{AB} = 22.7$ and $J_{AB} = 23.2$.

We used data from three fields observed in both J and K bands in the UKIDSS EDR, covering ~ 2900 , ~ 4500 and ~ 2900 arcmin 2 respectively. While exposure times are similar to the UDS EDR, the observing conditions are generally poorer. Direct comparison is also complicated by the different source extraction methods used by the DXS.

We applied the same selection method as described in Section 3.1, except that we did not visually inspect the samples. This selects 1523 objects in total, of which we estimate approximately 20 per cent are likely to be spurious (see Section 3.1), with a similar fraction likely to be artificially boosted due to photometric errors at faint magnitudes (Section 3.2). Since these errors are smaller than the errors in the DXS counts, for simplicity we opt not to make these corrections in our comparison with the UDS. We derive a median surface density of $n = 0.176 \pm 0.075$ arcmin $^{-2}$ at $K_{AB} = 21.2$, in very good agreement with the UDS value.

The resulting median counts from the three DXS samples are overplotted in Fig. 2, with errors representing the field-to-field rms variance. The agreement with UDS is very good. Although no corrections were applied, this crude comparison suggests that the density of DRGs is stable and broadly consistent between fields.

4 THE CLUSTERING OF DRGS

4.1 Angular clustering

In Fig. 3, we display the distribution of our sample of DRGs on the sky. Visually the DRGs appear strongly clustered. As a more quantitative measure, we evaluate the two-point angular correlation function, cutting our sample at $K_{AB} = 20.7$ as before.

To measure the angular correlation function $\omega(\theta)$ and estimate the related Poissonian errors we use the Landy & Szalay (1993) estimators. Fig. 4 shows the correlation function derived from our DRG sample. The best fit for the angular correlation is assumed to be a power law as

$$\omega(\theta) = A_\omega(\theta^{-\delta} - C_\delta),$$

with the amplitude at 1° $A_\omega = 3.1^{+2.1}_{-1.3} \times 10^{-3}$, the slope $\delta = 1.00 \pm 0.10$, and the integral constraint due to the limited area of the survey $C_\delta = 3.71$ (determined over the unmasked area).

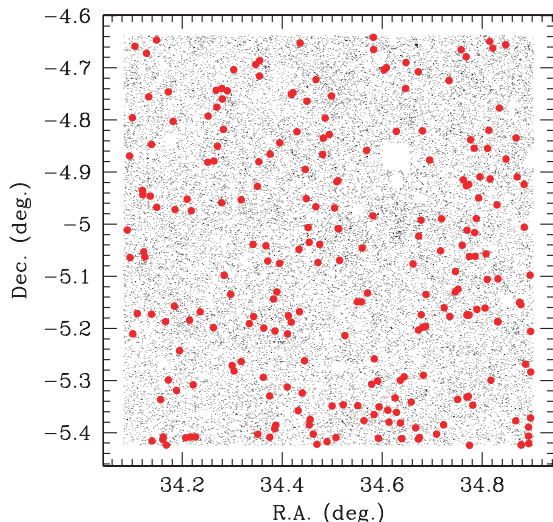


Figure 3. Distribution of our sample of DRGs on the sky, providing a visual impression of the large-scale structure. Small dots represent the full K -band galaxy sample, while larger symbols are the DRGs with $K_{AB} < 20.7$.

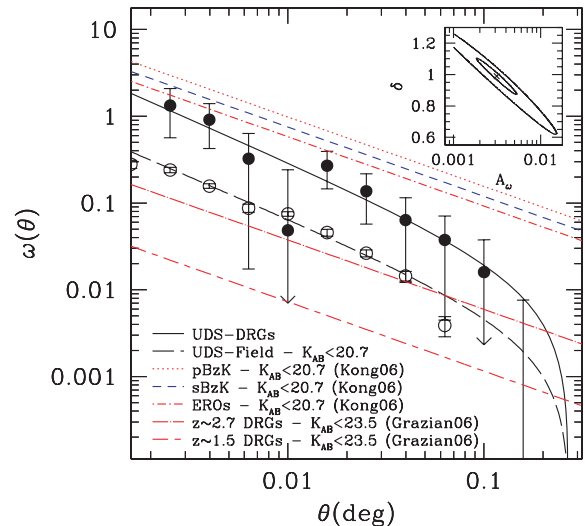


Figure 4. Two-point angular correlation function determined for our sample of DRGs (filled circles) and for the field galaxies (open circles) with $K_{AB} < 20.7$ and their fitted power laws. The plot inset presents the χ^2 minimization to estimate the best-fitting values of amplitude A_ω and slope δ for our sample of DRGs, with contours showing 1σ and 3σ confidence levels. For comparison, measurements from the literature for different samples are overplotted, assuming a slope of $\delta = 0.8$ (Kong et al. 2006; Grazian et al. 2006).

For comparison we also determine the angular correlation function for the full K -selected sample to a limiting magnitude of $K_{AB} < 20.7$, as shown in Fig. 4. The derived amplitude at 1° is $A_\omega = 8.1^{+2.3}_{-1.8} \times 10^{-4}$ for a slope of $\delta = 0.96 \pm 0.05$. Fixing the slope to the standard literature value ($\delta = 0.8$), we derive an amplitude of $A_\omega = 1.8^{+0.1}_{-0.1} \times 10^{-3}$ which is in good agreement with the work of Kong et al. (2006) to the same magnitude limit.

As shown in Fig. 4, by comparing with measurements from Kong et al. (2006) at the same magnitude limit of $K_{AB} < 20.7$, the amplitude of the DRG sample is ~ 5 times higher than that of field galaxies but a factor of ~ 2 lower than those of EROs and $(B - z)$ versus $(z - K)$ colour-colour selected (hereafter BzK-selected) galaxies. Interestingly, our derived clustering amplitude is notably higher than measurements for DRGs obtained by Grazian et al. (2006). This issue is explored further below.

4.2 Spatial correlation lengths and biasing

In order to compare the clustering of galaxy populations at different redshifts, we must derive spatial correlation measurements. Assuming a redshift distribution for our sample, we can derive the correlation length and a linear bias estimation using the relativistic Limber equation (Magliocchetti et al. 2000). The difficulty here is to have a realistic estimation of the redshift distribution of our sample. While Franx et al. (2003) have designed the $(J - K)_{AB} > 1.3$ criterion to select $z > 2$ galaxies, Grazian et al. (2006) and Conselice et al. (2006) have shown that the redshift distribution is broad, and the fraction of $z < 2$ galaxies increases at bright magnitudes.

As a preliminary investigation we assume a Gaussian form for the redshift distribution, fixing the mean and standard deviation to match recent studies of fainter DRGs. Analytical and fitted redshift distributions make no significant difference to our derived correlation lengths. The correlation length can then be evaluated if we fix the slope of the correlation function to $\gamma = 1 + \delta = 2.0$. In the

DRG sample of Grazian et al. (2006), a mean redshift of $\bar{z} = 1.5$ was found at a limit of $K_{AB} < 22.0$. Using this mean redshift with $\sigma = 0.5$ (broadly matching their distribution), we determine $r_0 = 14.1^{+4.8}_{-2.9} h^{-1}$ Mpc and $b = 4.8^{+1.7}_{-1.1}$ for our DRGs. Conselice et al. (2006) suggest that very bright DRGs lie at even lower redshifts. If we adopt the observed redshift distribution of their spectroscopic sample, we derive $r_0 = 11.0^{+3.7}_{-2.3} h^{-1}$ Mpc and $b = 4.0^{+1.4}_{-0.8}$, when the approximated Gaussian form gives (with $\bar{z} = 1.0$ and $\sigma = 0.25$) $r_0 = 11.1^{+3.8}_{-2.3} h^{-1}$ Mpc and $b = 4.0^{+1.4}_{-0.8}$.

Grazian et al. (2006) also split their sample according to redshift, and found $r_0 = 7.4^{+3.5}_{-4.9} h^{-1}$ Mpc for DRGs at $1 < z < 2$ with $K_{AB} < 22$. Our sample is substantially brighter, so, even if the two samples are probing slightly different redshifts, our larger correlation length could be interpreted as evidence for luminosity segregation, e.g. we may be sampling more luminous galaxies which are more strongly biased (Pollo et al. 2006). We note that Quadri et al. (2006) find no relationship between K -magnitude and correlation length for K -selected galaxies, but instead find a strong relationship between colour and correlation length (with redder galaxies being more strongly clustered). This is not inconsistent with our findings, since we are studying segregation *within* a colour-selected sample.

As shown in Fig. 4, our measurement is comparable to the clustering of EROs or BzK-selected galaxies at the same limiting magnitude, which are likely to sample a similar redshift distribution to our DRGs, and hence show similar correlation lengths. Overzier et al. (2003) compared the clustering of EROs with predictions of dark matter halo models. Adopting the same technique, we can infer that bright DRGs are likely to be hosted by very massive dark matter haloes (possibly $M > 10^{14} M_{\odot}$), consistent with the potential progenitors of present-day $L \gtrsim L_*$ elliptical galaxies.

Finally we note that while the slope of our angular correlation function is steep, the fiducial value of $\delta = 0.8$ is only excluded by our sample at a 1σ level. Further data will be required to investigate whether this may be caused by a possible transition between inner and outer halo occupation numbers (e.g. Ouchi et al. 2005).

5 SUMMARY

We have extracted a large sample of bright DRGs from the UKIDSS UDS EDR. Our catalogue contains 369 DRGs to a limiting magnitude of $K_{AB} = 21.2$, extracted over an area of 0.62 deg^2 . The fainter $K_{AB} > 20.0$ number counts are in good agreement with previous estimates, while at brighter magnitudes the sample is unique. Using simulations we have determined that contamination due to photometric errors is below ~ 16 per cent at an approximate completeness limit of $K_{AB} < 20.7$.

From this sample we have extracted a sub-sample of 239 bright DRGs to a limit of $K_{AB} = 20.7$. These bright DRGs appear highly clustered, and we determine a correlation length of $r_0 \simeq 11 h^{-1}$ Mpc and a bias measurement $b \simeq 4.5$, assuming that the sample lies at a mean redshift of $\bar{z} = 1.0$ with a standard deviation of $\sigma = 0.25$ (consistent with studies at similar depths – Conselice et al. 2006).

They appear more clustered than fainter samples of DRGs derived at these redshifts, which may be evidence for luminosity segregation, in agreement with biased galaxy formation scenarios.

ACKNOWLEDGMENTS

The authors thank the referee for a detailed and thorough report which improved the paper, Stephen Warren and Stephen Serjeant for their useful comments, and Nigel Hambly and Nick Cross for their help with data reduction. We are also grateful to the staff at UKIRT for making these observations possible, and acknowledge the Cambridge Astronomical Survey Unit and the Wide Field Astronomy Unit in Edinburgh for processing the UKIDSS data. SF, CS and MC acknowledge funding from PPARC. OA, IS and RJM acknowledge the support of the Royal Society.

REFERENCES

- Bertin E., Arnouts S., 1996, *A&A*, 117, 393
 Bertin E., Mellier Y., Radovich M., Missonier G., Didelon P., Morin B., 2002, in Bohlender D. A., Durand D., Handley T. H., eds, *ASP Conf. Ser.*, Vol. 281, *Astronomical Data Analysis Software and Systems XI*. Astron. Soc. Pac., San Francisco, p. 228
 Conselice C. J. et al., 2006, *ApJ*, in press (astro-ph/0607242)
 Daddi E. et al., 2003, *ApJ*, 588, 50
 Dye S. et al., 2007, *MNRAS*, 372, 1227
 Förster Schreiber N. M. et al., 2004, *ApJ*, 616, 40
 Franx M. et al., 2003, *ApJ*, 587, L79
 Gardner J. P., Cowie L. L., Wainscoat R. J., 1993, *ApJ*, 415, L9
 Gehrels N., 1986, *ApJ*, 303, 336
 Grazian A. et al. 2006, *A&A*, submitted (astro-ph/0603095)
 Kong X. et al., 2006, *ApJ*, 638, 72
 Labbé I. et al., 2003, *AJ*, 125, 1107
 Labbé I. et al., 2005, *ApJ*, 624, L81
 Landy S. D., Szalay A. S., 1993, *ApJ*, 412, 64
 Lawrence A. et al., 2006, *MNRAS*, submitted (astro-ph/0604426)
 Magliocchetti M., Bagla J. S., Maddox S. J., Lahav O., 2000, *MNRAS*, 314, 546
 Ouchi M. et al., 2005, *ApJ*, 635, L117
 Overzier R. A., Röttgering H. J. A., Rengelink R. B., Wilman R. J., 2003, *A&A*, 405, 53
 Pollo A. et al., 2006, *A&A*, 451, 409
 Quadri R. et al. 2006, *ApJ*, submitted (astro-ph/0606330)
 Reddy N. A., Erb D. K., Steidel C. C., Shapley A. E., Adelberger K. L., Pettini M., 2005, *ApJ*, 633, 748
 Rudnick G. et al., 2003, *ApJ*, 599, 847
 Sekiguchi K. et al., 2005, in Bender R., Renzini A., eds, *Multiwavelength Mapping of Galaxy Formation and Evolution*, p. 82
 Steidel C. C., Giavalisco M., Dickinson M., Adelberger K. L., 1996, *AJ*, 112, 352
 van Dokkum P. G. et al., 2003, *ApJ*, 587, L83

This paper has been typeset from a $\text{\TeX}/\text{\LaTeX}$ file prepared by the author.